JOC Article

The Preference for Anti over Gauche Migration in the Baeyer−Villiger Reaction

Michelle Snowden,[†] Amy Bermudez,[†] David R. Kelly,[‡] and Jennifer L. Radkiewicz-Poutsma*,[†]

Department of Chemistry and Biochemistry, Old Dominion University, 4541 Hampton Boulevard, Norfolk, Virginia 20529, and School of Chemistry, Cardiff University, P.O. Box 912, Cardiff CF10 3TB, Wales, United Kingdom

jradkiew@odu.edu

Received May 24, 2004

Explanations for stereoselectivity in the Baeyer−Villiger reaction have relied on the assumption that the antiperiplanar (*app*) group migrates. However, the magnitude of the preference for *app*-migration over gauche migration is unknown. To investigate this, the energy differences between the two were estimated from ab initio calculations. *App*-migration was found to be the preferred pathway since no transition structure could be located for gauche migration. Barriers for gauche migration were estimated by performing constrained optimizations. *App*-migration was found to be strongly favored with a barrier that is at least 3.8 kcal/mol and as much as 58.0 kcal/mol lower in energy than the gauche migration barrier.

Introduction

The Baeyer−Villiger reaction is the oxidation of a ketone to an ester or lactone by a peroxide.[1] In the laboratory, percarboxylic acids are commonly used as the peroxide reagent whereas on an industrial scale hydrogen peroxide with a catalyst is preferred on the grounds of cost and process intensification. The reaction has considerable industrial importance for the manufacture of fine chemicals, in particular, lactones, which are key fragrance ingredients. Until the mid-1990s, the only asymmetric form of the reaction was that catalyzed by flavoenzymes,[2−4] but in 1994, the first two reports of asymmetric metal-catalyzed Baeyer−Villiger reactions appeared in the literature.[5,6] Since then, various cobalt-,[7] copper-,[8] palladium-,[9] platinum-,[10] and zirconium-complexes,[11] aluminum-[12] and magnesium-BINOL complexes,[13] titanium alkoxides,[14] diselenides,[15] and bisflavin[16] catalysts[17] have been developed which show fair to excellent enantioselectivities.[18] Enantioselective Baeyer−Villiger oxidation by stoichiometric TADDOL hydroperoxide has provided a useful study of the mechanism.[19] The flavoenzyme-catalyzed reaction has been improved by the isolation of new organisms with Baeyer−Villigerase activity,[20] expression in easily cultivated organisms such as yeast,[3,21] and the optimization of process parameters (e.g. oxygenation) to enable manufacture on a large scale.[22] The combination of lipases with hydrogen peroxide provides a unique alternative to flavoenzymes.[23]

The mechanism of all Baeyer−Villiger reactions involves nucleophilic addition of the peroxide reagent to

* Address correspondence to this author.
[†] Old Dominion University.
[‡] Cardiff University.

(1) Reviews: for a historical and mechanistic perspective: Renz, M.; Meunier, B. *Eur. J. Org. Chem.* **1999**, 737−750. For a compilation of examples see: Krow, G. R. *Org. React.* **1993**, *43*, 251−798.
(2) Mihovilovic, M. D.; Muller, B.; Stanetty, P. *Eur. J. Org. Chem.* **2002**, 3711−3730. Roberts, S. M.; Wan, P. W. H. *J. Mol. Catal. B* **1998**, *4*, 111.
(3) Stewart, J. D. *Curr. Org. Chem.* **1998**, *2*, 195.
(4) The reactive intermedaite is a 4a-flavin hydroperoxide: Sheng, D. W.; Ballou, D. P.; Massey, V. *Biochemistry* **2001**, *40*, 11156−11167.
(5) Gussa, A.; Baccin, C.; Pinna, F.; Strukul, G. *Organometallics* **1994**, *13*, 3442−3451.
(6) Bolm, C.; Schlingloff, G.; Weickhardt, K. *Angew. Chem., Int. Ed.* **1994**, *106*, 1944−1946.
(7) Uchida, T.; Katsuki T.; Ito, K.; Akashi, S.; Ishii, A.; Kuroda, T. *Helv. Chim. Acta* **2002**, *85*, 3078−3089.
(8) Bolm, C. In *Advances in Catalytic Processes*; JAI Press Inc.: Stamford, CT, 1997; Vol. 2, pp 43−68; Bolm, C.; Luong, T. K. K.; Schlingloff, G. *Synlett* **1997**, *10*, 1151−1152.
(9) Ito, K.; Ishii, A.; Kuroda, T.; Katsuki, T. *Synlett* **2003**, *5*, 643−646.
(10) Brunetta, A.; Strukul, G. *Eur. J. Inorg. Chem.* **2004**, 1030−1038.
(11) Watanabe, A.; Uchida, T.; Irie, R.; Katsuki, T. *Proc. Natl. Acad. Sci.* **2004**, *101*, 5737−5742. Bolm, C.; Beckmann, O. *Chirality* **2000**, *12*, 523−526.
(12) Bolm, C.; Beckmann, O.; Palazzi C. *Can. J. Chem.* **2001**, *79*, 1593−1597.
(13) Bolm, C.; Beckmann, O.; Cosp, A.; Palazzi, C. *Synlett* **2001**, 1461−1463.
(14) Kanger, T.; Kriis, K.; Paju, A.; Pehk, T.; Lop, M. *Tetrahedron: Asymmetry* **1998**, *9*, 4475−4482.
(15) Miyake, Y.; Nishibayashi, Y.; Uemura, S. *Bull. Chem. Soc. Jpn.* **2002**, *75*, 2233−2237.
(16) Murahashi, S. I.; Ono, S.; Imada, Y. *Angew. Chem., Int. Ed.* **2002**, *41*, 2366−2368.
(17) For a review of transition metal catalyzed Baeyer−Villiger reactions see: Strukul, G. *Angew. Chem., Int. Ed.* **1998**, *37*, 1198.
(18) For a comparison of flavoenzyme and metal complex catalyzed asymmetric Baeyer−Villiger reactions see: Kelly D. R. *Chimica Oggi* **2000**, *18*, 33−37, 52−56.
(19) Aoki, M.; Seebach, D. *Helv. Chim. Acta* **2001**, *84*, 187−207.
(20) Mihovilovic, M. D.; Rudroff, F.; Müller, B.; Stanetty, P. *Bioorg. Med. Chem. Lett.* **2003**, *13*, 1479−1482.
(21) Kyte, B. G.; Rouvière, P.; Cheng, Q.; Stewart, J. D. *J. Org. Chem.* **2004**, *69*, 12−17.
(22) Alphand, V.; Carrea, G.; Wohlgemuth, R.; Furstoss, R.; Woodley, J. M. *Trends Biotechnol.* **2003**, *21*, 318−323.
(23) Pchelka, B. K.; Gelo-Pujic, M.; Guibe-Jampel, E. *J. Chem. Soc., Perkin Trans. 1* **1998**, 2625.

10.1021/jo0491307 CCC: $27.50
Published on Web 09/21/2004

SCHEME 1. The Criegee Mechanism for the Baeyer−Villiger Reaction[a]

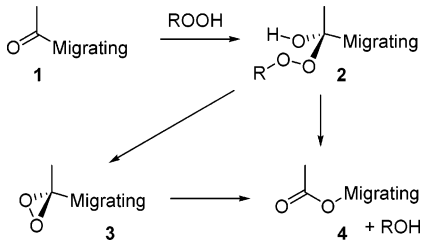

[a] The Criegee intermediate **2** is represented here as a hydroxy peroxide, but with appropriate catalysts the hydroxyl group may be present as a metal alkoxide or engaged in a hemiacetal, orthoacid, or orthoamide group, etc.

the carbonyl group to give the tetrahedral Criegee intermediate **2**. In the Criegee mechanism, this undergoes intramolecular migration of a substituent from carbon to oxygen with cleavage of the peroxide bond and simultaneous loss of RO^- to give an ester or lactone **4**. The rearrangement step is usually, but not always, rate limiting, and the rate of rearrangement is enhanced by electron-withdrawing groups on the peroxide.[24] In both the percarboxylic acid[25] and flavoenzyme[26] mediated reactions the group that migrates does so with retention of configuration. With reagents that bear strongly electron-withdrawing groups (e.g. $Me_3SiOOSO_3SiMe_3$[27] and Caro's acid, which was used by Baeyer and Villiger) the Criegee intermediate **2** undergoes ring closure to give a dioxirane **3**, which in turn rearranges to an ester or lactone. Baeyer and Villiger correctly postulated dioxiranes some 80 years before they were isolated. It is interesting to note that although Baeyer and Villiger discovered the first percarboxylic acid, perbenzoic acid, they never used it in the reaction that bears their name! A verifiable consequence of the Criegee mechanism is that the carbonyl oxygen of the ester or lactone **3** is derived from the carbonyl oxygen of the ketone **1**, and the intraannular oxygen is derived from the peroxide reagent. This has been demonstrated for both the percarboxylic acid[28] and flavoenzyme[29] variants of the reaction, which also excludes the dioxirane mechanism under these conditions.[30]

The origin of the regioselectivity of Baeyer−Villiger reactions has been disputed almost since the discovery of the reaction. It was quickly noticed that the ease of migration of a group is in the same rank order as the ability of the migrating group to stabilize a carbocation, e.g. *tert*-butyl > isopropyl > methyl; however, the rate differences barely span 2 orders of magnitude, whereas the differences in carbocation stability as measured by rates of solvolysis are 6−8 orders of magnitude.[31] The crucial study in support of the carbocation mechanism was an investigation of differently para-substituted benzophenones, which showed that electron-rich phenyl groups (e.g. $CH_3OC_6H_4^-$) migrated in preference to those bearing electron-withdrawing groups (e.g. $NO_2C_6H_4^-$).[32] However, the regioselectivity of Baeyer−Villiger oxidation of bicyclic ketones[33−35] is predicted rather poorly by the carbocation argument.[36] Stereochemical arguments for rationalizing the regiochemistry of the Baeyer−Villiger reaction were made as early as the 1950s, but the arguments are difficult to apply, because no Criegee intermediate[37] has ever been isolated and hence it has only been possible to infer the diastereoselectivity of addition and the conformation from the regiochemistry of oxygen insertion. The first evidence for a wholly stereoelectronically controlled migration was an intramolecular Baeyer−Villiger reaction, in which a methylene group migrated in preference to a methine group.[38] This result was largely overlooked until results from flavoenzyme catalyzed enantioselective Baeyer−Villiger reactions necessitated reexamination of the mechanism. In brief summary, these reactions are highly enantioselective and the regiochemistry observed does not match prior results with percarboxylic acids. For example, the enantiomeric ketones **5** and **6** gave the regioisomeric lactones **7** and **8** with high enantiomeric excesses and in good yields, whereas in the percarboxylic acid-catalyzed reactions, the lactone **7** (and *ent*-**7**) is always the predominant product.

The stereochemical course of the flavoenzyme-catalyzed Baeyer−Villiger oxidation of the bicyclic ketones **5**, **6** was rationalized as binding of the two enantiomers at the active site, with different orientations, such that migration occurred at similarly disposed bonds, i.e., 5,6 and 6,7, respectively. This was confirmed by the synthesis of the superimposition mimic **9**, which also underwent ring expansion to give the lactone **10** (or *ent*-**10**) in the same sense with five highly purified flavoenzymes[39,40] and several metal catalysts, Pd(II),[9] Co(III),[7] Cu(II),[8] and selenium[15] (91−99% ee). An additional benefit of using ketone **9** as a substrate is that attack by the hydroperoxide can confidently be predicted to occur exclusively

(24) Hawthorne, M. F.; Emmons, W. D. *J. Am. Chem. Soc.* **1958**, *80*, 6398−6404.
(25) Rozzell, J. D.; Benner, S. A. *J. Org. Chem.* **1983**, *48*, 1190−1193 and references therein.
(26) Schwab, J. M.; Li, W.; Thomas, L. P. *J. Am. Chem. Soc.* **1983**, *105*, 4800−4808, 3614.
(27) Camporeale, M.; Fiorani, T.; Troisi, L.; Adam, W.; Curci, R.; Edwards, J. O. *J. Org. Chem.* **1990**, *55*, 93−98.
(28) Doering, W. v. E.; Dorfman, E. *J. Am. Chem. Soc.* **1953**, *75*, 5595−5598. Bunton, C. A.; Lewis, T. A.; Llewellyn, D. R. *J. Chem. Soc.* **1956**, 1226.
(29) Praire, R. L.; Talalay, P. *Biochemistry* **1963**, *2*, 203. Britton, L. N.; Brand, J. M.; Markovetz, A. J. *Biochim. Biophys. Acta* **1974**, *369*, 45.
(30) Evidence has been reported recently for a third mechanism that proceeds via a spirobisperoxide: Berkessel, A.; Andreae, M. R. M.; Schmickler, H.; Lex, J. *Angew. Chem., Int. Ed.* **2002**, *41*, 4481−4483.
(31) Hawthorne, M. F.; Emmons, W. D. *J. Am. Chem. Soc.* **1958**, *80*, 6393−6398.
(32) Doering, W. v. E.; Speers, L. *J. Am. Chem. Soc.* **1950**, *75*, 5515−5518. Mitsuhashi, T.; Miyadera, H.; Simamura, O. *J. Chem. Soc., Chem. Commun.* **1970**, 1301−1302.
(33) Grudzinski, Z.; Roberts, S. M.; Howard, C.; Newton, R. F. *J. Chem. Soc., Perkin Trans. 1* **1978**, 1182.
(34) Hamley, P.; Holmes, A. B.; Marshall, D. R.; MacKinnon, J. W. M. *J. Chem. Soc., Perkin Trans. 1* **1991**, 1793.
(35) Harmata, M.; Rashatasakhon, P. *Tetrahedron Lett.* **2002**, *43*.
(36) Noyori, R.; Kobayashi, H.; Sato, T. *Tetrahedron Lett.* **1980**, 2573. Noyori, R.; Sato, T.; Kobayashi, H. *Bull. Chem. Soc. Jpn.* **1983**, *56*, 2661−2679.
(37) α-Hydroxy-hydroperoxides are stable, if the substituents bear electron-withdrawing groups (e.g., CF_3). Ganeshpure, P. A.; Adam, W. *Synthesis* **1996**, 179−188.
(38) Chandrasekfar, S.; Roy, C. D. *J. Chem. Soc., Perkins Trans. 2* **1994**, 2141.
(39) Kelly, D. R.; Knowles, C. J.; Mahdi, J. G.; Taylor, I. N.; Wright, M. A. *J. Chem. Soc., Chem. Commun.* **1995**, 729. Kelly, D. R.; Knowles, C. J.; Mahdi, J. G.; Wright, M. A.; Taylor, I. N.; Hibbs, D. E.; Hursthouse, M. B.; Mish'al, A. K.; Roberts, S. M.; Wan, P. W. H.; Grogan, G.; Willetts, A. J. *J. Chem. Soc., Perkin Trans. 1* **1995**, 2057.
(40) Kelly, D. R.; Knowles, C. J.; Mahdi, J. G.; Wright, M. A.; Taylor, I. N.; Roberts, S. M.; Wan, P. W. H.; Grogan, G.; Pedragosa-Moreau, S.; Willetts, A. J. *J. Chem. Soc., Chem. Commun.* **1996**, 2333.

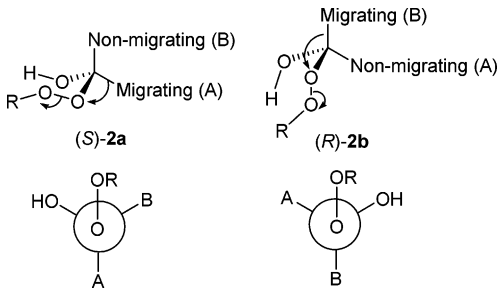

FIGURE 1. In conformer **2a**, group A migrates, and in **2b**, B migrates. The catalyst stabilizes either **2a** or **2b**. The conformations can be interconverted by rotation about the O−C bond. R is acyl, alkyl, or flavin.

SCHEME 2. Congruent Enantioselective Baeyer−Villiger Oxidation

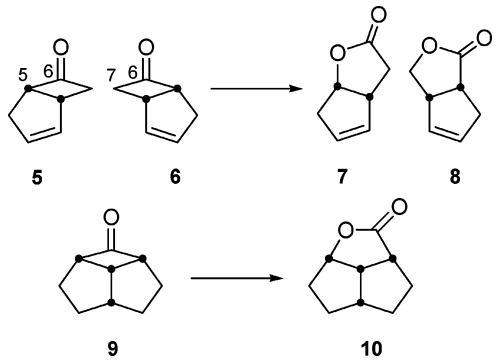

from the *exo*-face.[39] Given that the diastereofacial selectivity of the attack of the ketone by the hydroperoxide and the regiochemistry of ring expansion are known, the stereochemistry of the Criegee intermediate can be deduced from stereoelectronic principles (Figure 1). Using the Cahn−Ingold−Prelog convention and assigning the migrating group a higher priority than the nonmigrating group can conveniently distinguish the two possible intermediates. The central tenet of the stereoelectronic model for enantioselective Baeyer−Villiger reactions is that all reactions of a given enantiomerically pure catalyst or reagent proceed via a single Criegee intermediate of the same absolute stereochemistry as defined above.[18] For example, the stereoselectivity shown in Scheme 2 arises from the (*S*)-**2a** Criegee intermediate.

The terms (*S*) and (*R*) applied to the Criegee intermediates **2a**, **2b** are surrogates for descriptions of the orientation of the peroxide bond relative to the migrating and nonmigrating groups. It is assumed that the orientation of the peroxide bond is antiperiplanar to that of the migrating group, so that the σ bonding orbital of the migrating group and the σ^* antibonding orbital of the peroxide bond overlap (Figure 2). This assumption has been made numerous times and has been described as the *primary stereoelectronic effect*.[41] This has played a key role in the interpretation of recent studies of the Baeyer−Villiger oxidation of *cis*-4-*tert*-butyl-2-fluorocyclohexanone, where the fluorosubstituted methylene migrates in preference to the unsubstituted methylene,[42] contrary

(41) The conformation of the hydroxyl group is potentially the origin of another stereoelectronic effect.[43]

(42) Crudden, C. M.; Chen, A. C.; Calhoun, L. A. *Angew. Chem., Int. Ed.* **2000**, *39*, 2852−2855.

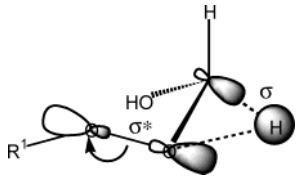

FIGURE 2. $\sigma-\sigma^*$ interaction between the bonding orbital of the C−H bond and the antibonding orbital of the O−O bond in the Baeyer−Villiger oxidation of formaldehyde to formic acid.

to the preferences of 2-trifluoromethylcyclohexanone,[43] acyclic fluorinated ketones,[44] and the carbocation rationalization. Similarly, the preference for antiperiplanar migration in the Criegee rearrangement of allylic peroxides has been successfully predicted from the conformation of the hydroperoxides in the crystalline state.[45] It is also the basis of a model for the flavoenzyme-catalyzed Bayer−Villiger oxidation, in which engaging the hydroxyl group in an orthoamide controls the stereochemistry of the Criegee intermediate.[46]

The catalyst is presumed to stabilize one of two possible conformations, **2a** or **2b**. This restricts one of the two possible migratory groups (A or B) to the antiperiplanar position (Figure 1). Assuming that the addition of the peroxide to the ketone is stereoselective and that the catalyst binds only one conformation of the intermediate (either **2a** or **2b**), only one enantiomeric product should be observed. If both the antiperiplanar and gauche bonds (A and B in **2a**) migrated to the same extent, there would be no stereoselectivity. However, the energetic difference between gauche and antiperiplanar transfer is unknown, and so the degree of preference arising from stereoelectronic factors is unknown. We have explored the relationships between the conformation of peroxide intermediates in this reaction and the degree of selectivity in alkyl group migration using quantum mechanical methods. The results predict a high preference for antiperiplanar migration that dictates the regioselectivity of the reaction.

Methodology

We have employed ab initio RHF and DFT calculations with the B3LYP functional to predict the energy difference between antiperiplanar and gauche migration. Previous calculations on this reaction reported in the literature only include antiperiplanar migrations,[47−50] and most were performed with semiempirical or low levels of theory.[51−54] None of these studies

(43) Itoh, Y.; Yamanaka, M.; Mikami, K. *Org. Lett.* **2003**, *5*, 4803−4806.

(44) Kitazume, T.; Kataoka, J. *J. Fluorine Chem.* **1996**, *80*, 157−158. Kobayashi, S.; Tanaka, H.; Amii, H.; Uneyama, K. *Tetrahedron* **2003**, *59*, 1547−1552.

(45) Goodman, R. M.; Kishi, Y. *J. Am. Chem. Soc.* **1998**, *120*, 9392.

(46) Kelly D. R. *Tetrahedron*: *Asymmetry* **1996**, *7*, 1149−1152.

(47) Cardenas, R.; Cetina, R.; Lagunez-Otero, J.; Reyes, L. *J. Phys. Chem. A* **1997**, *101*, 192.

(48) Okuno, Y. *Chem. Eur. J.* **1997**, *3*, 212.

(49) Lehtinen, C.; Nevalainen, V.; Brunow, G. *Tetrahedron* **2000**, *56*.

(50) Carlqvist, P.; Eklund, R.; Brinck, T. *J. Org. Chem.* **2001**, *66*, 1193−1199.

(51) Stoute, V. A.; Winnik, M. A.; Csizmadia, I. G. *J. Am. Chem. Soc.* **1974**, *96*, 6388.

(52) Rubio, M.; Cetina, R.; Bejarano, A. *Afinidad* **1983**, 185.

(53) Hannachi, H.; Anoune, N.; Arnaud, C.; Lanteri, P.; Longeray, R.; Chermette, H. *J. Mol. Struct.* **1998**, *434*, 183.

SCHEME 3

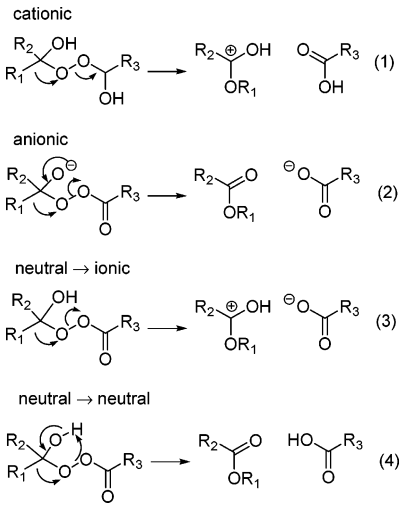

mention the possibility of gauche transition states or even that a search was made to locate them. Gaussian 94[55] and Gaussian 98[56] optimizations at the RHF/6-31G* and B3LYP/6-311G* levels of theory were performed. For all nonconstrained structures, frequencies were calculated to confirm the nature of stationary points.

The Criegee intermediate of the Baeyer−Villiger reaction can either be charged or neutral, depending on the reaction conditions. Migration from an ionic intermediate gives a neutral product plus an ionic product (Scheme 3, eqs 1 and 2). Migration from a neutral intermediate gives a cationic ester and an anionic carboxylic acid, or with simultaneous intramolecular proton transfer, a neutral ester and carboxylic acid (Scheme 3, eqs 3 and 4). Previously, gas-phase calculations have only been performed on neutral intermediates resulting in neutral products.[49,50,57] In most cases, a neutral intermediate to charged products reaction is unstable in the gas phase and the corresponding transition structures are not stationary points. In solution, it is expected that the BV reaction is ionic or that a neutral intermediate rearranges to ionic products. Because the neutral-to-neutral migration is not representative of solution behavior and neutral-to-charged calculations are not possible, only ionic model systems of the BV reaction were employed.

Results and Discussion

The cationic and anionic rearrangements were modeled by four different systems: formaldehyde plus hydrogen peroxide (**11** and **15**), acetaldehyde plus hydrogen peroxide (**12** and **16**), formaldehyde plus peroxyformic acid (**13** and **17**), and acetaldehyde plus peroxyformic acid (**14** and **18**) (Scheme 4). For the cationic systems **13** and **14**, the peroxyformic carbonyl oxygen is protonated. Previous calculations have shown that intermediates cannot be located when the system is protonated on the peroxy oxygen.[47]

SCHEME 4

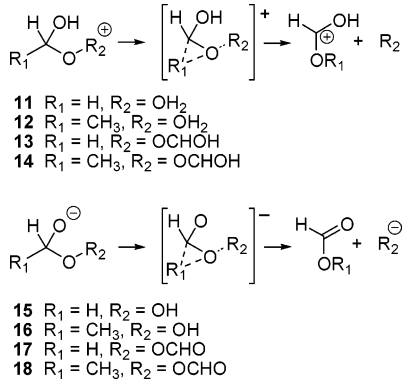

All attempts to locate a transition state for the nonantiperiplanar (gauche) transition structure were unsuccessful. Qualitatively, this indicates the unfavorable nature of gauche migration. It was noticed that many of the structures used to try and locate a gauche transition structure optimized to a constrained syn-migration transition structure, but a syn-migration TS could not be located. Moreover, in current models for metal complex[17] and flavoenzyme[18,46] catalyzed asymmetric Baeyer−Villiger reactions, syn-geometry is not geometrically feasible.

The energy barrier for gauche migration was estimated by performing two sets of constrained optimizations. In the first system (gauche TS1), calculations were started from reactant structures. In the cases of R_1 = Me (Scheme 4), the methyl group was gauche to the O−O bond. The bond angle of the antiperiplanar hydrogen (H−C−O) was constrained to the reactant value to prevent *app*-H migration. The peroxide bond was then stretched incrementally to simulate the breaking of this bond until the structure could no longer be optimized or the energy reached a maximum. Gauche hydrogen or methyl transfer was not observed in any of these structures. In some cases, stretching of the peroxide bond led to immediate rearrangement or breaking of the carbon−oxygen bond. For these structures a reliable gauche TS1 estimate could not be obtained. For the second system (gauche TS2), the gauche hydrogen was held in the transition state geometry obtained from the anti-migration. This meant that the O−O, O−C, and gauche-H−C (or gauche-C−C) bond lengths and the O−C−gauche-H (or O−C−gauche-C) bond angle were frozen. In addition, the O−O−C−*app*-H dihedral angle was also constrained to prohibit rotation about the O−C bond.

Dihedral scans were performed at the RHF/6-31G* level of theory to ensure that all-important conformers were located. The total and relative energies for all located conformers and transition structures are provided in the Supporting Information. Only select conformers were recalculated at the B3LYP/6-311G* level of theory. For each model system, the lowest energy conformer and

(54) Cadenas, R.; Reyes, L.; Lagunez-Otero, J.; Cetina, R. *J. Mol. Struct.* **2000**, *497*, 211.

(55) Frisch, M. J.; Trucks, G. W.; Schlegel, H. B.; Gill, P. M. W.; Johnson, B. G.; Robb, M. A.; Cheeseman, J. R.; Keith, T.; Petersson, G. A.; Montgomery, J. A.; Raghavachari, K.; Al-Laham, M. A.; Zakrzewski, V. G.; Ortiz, J. V.; Foresman, J. B.; Cioslowski, J.; Stefanov, B. B.; Nanayakkara, A.; Challacombe, M.; Peng, C. Y.; Ayala, P. Y.; Chen, W.; Wong, M. W.; Andres, J. L.; Replogle, E. S.; Gomperts, R.; Martin, R. L.; Fox, D. J.; Binkley, J. S.; Defrees, D. J.; Baker, J.; Stewart, J. P.; Head-Gordon, M.; Gonzalez, C.; Pople, J. A. *Gaussian 94*; Gaussian, Inc.: Pittsburgh, PA, 1995.

(56) Frisch, M. J.; Trucks, G. W.; Schlegel, H. B.; Scuseria, G. E.; Robb, M. A.; Cheeseman, J. R.; Zakrzewski, V. G.; Montgomery, J. A.; Stratmann, R. E.; Burant, J. C.; Dapprich, S.; Millam, J. M.; Daniels, A. D.; Kudin, K. N.; Strain, M. C.; Farkas, O.; Tomasi, J.; Barone, V.; Cossi, M.; Cammi, R.; Mennucci, B.; Pomelli, C.; Adamo, C.; Clifford, S.; Ochterski, J.; Petersson, G. A.; Ayala, P. Y.; Cui, Q.; Morokuma, K.; Malick, D. K.; Rabuck, A. D.; Raghavachari, K.; Foresman, J. B.; Cioslowski, J.; Ortiz, J. V.; Stefanov, B. B.; Liu, G.; Liashenko, A.; Piskorz, P.; Komaromi, I.; Gomperts, R.; Martin, R. L.; Fox, D. J.; Keith, T.; Al-Laham, M. A.; Peng, C. Y.; Nanayakkara, A.; Gonzalez, C.; Challacombe, M.; Gill, P. M. W.; Johnson, B. G.; Chen, W.; Wong, M. W.; Andres, J. L.; Head-Gordon, M.; Replogle, E. S.; Pople, J. A. *Gaussian 98*; Gaussian, Inc.: Pittsburgh, PA, 1998.

(57) Sever, R. R.; Root, T. W. *J. Phys. Chem. B* **2003**, *107*, 10848−10862.

TABLE 1. RHF/6-31G* Relative Energies (kcal/mol) for the Baeyer−Villiger Cationic Reaction for Various Model Systems

	11		12		13		14	
compd	rel *E*	TS Δ*E*	rel *E*	TS Δ*E*	rel *E*	TS Δ*E*	rel *E*	TS Δ*E*
reactant	0.0		0.0		0.0		0.0	
antiperiplanar TS	21.9	0.0	18.7	0.0	30.2	0.0	27.2	0.0
product complex	−105.9		−98.6		−93.4		−85.4	
gauche TS model 1	33.8	11.9	32.5	13.8	44.9	14.7	39.9	12.7
gauche TS model 2	63.3	41.4	60.8	42.1	75.0	44.8	71.2	44.0

TABLE 2. B3LYP/6-311G* Relative Energies (kcal/mol) for the Baeyer−Villiger Cationic Reaction for Various Model Systems

	11		12		13		14	
compd	rel *E*	TS Δ*E*	rel *E*	TS Δ*E*	rel *E*	TS Δ*E*	rel *E*	TS Δ*E*
reactant	0.0		0.0		0.0		0.0	
antiperiplanar TS	1.4	0.0	2.6	0.0	8.3	0.0	7.3	0.0
product complex	−101.3		−91.6		−88.6		−76.9	
gauche TS model 1	9.3	7.9	4.2	1.6	22.6	14.3	11.9	4.6
gauche TS model 2	20.3	18.9	16.6	14.0	42.1	33.8	28.9	21.6

the conformers with the lowest *app*-migration barrier, gauche TS1 barrier, or gauche TS2 barrier with respect to the lowest energy conformer were chosen. In addition the barriers were determined for each conformer, i.e., Δ*E* of A to TSA, and the conformers with the lowest *app*-migration barrier, gauche TS1 barrier, or gauche TS2 barrier were also recalculated at the higher level of theory. In many cases, the same conformer met several of the above criteria. The total and relative energies for these conformers are also provided in the Supporting Information.

Cationic Baeyer−Villiger Rearrangement. The results from the RHF/6-31G* and B3LYP/6-311G* calculations for the cationic model systems are given in Tables 1 and 2, respectively. Figure 3 contains the B3LYP/6-311G* cationic geometries of the reactant, the antiperiplanar transition structure, the product complex, the gauche TS1 model, and the gauche TS2 model for acetaldehyde plus peroxyformic acid, **14**. Of most importance is the energy difference between the barriers for *app*-migration and the estimated barriers for gauche migration. The *app*-migration barrier ranges from 18.7 kcal/mol for **12** to 30.2 kcal/mol for **13**. The inclusion of correlation energy has a large effect, resulting in lower barriers, which are now 1.4 (**11**) to 8.3 kcal/mol (**13**). Consequently, the DFT *app* structures occur via an earlier transition state than the corresponding RHF structures as determined by the extent of bond breaking and bond formation. Note that for model systems **11** and **12**, there is essentially no barrier for *app*-migration.

Using the first method to estimate the gauche migration transition structure gave barriers that ranged from 32.5 (**12**) to 44.9 kcal/mol (**13**) and O−O bond lengths of ∼2.0 Å. The DFT barriers were 4.2 (**12**) to 22.6 kcal/mol (**13**), with O−O bond lengths of 2.3 Å for **11**, 2.1 Å for **12**, 2.5 Å for **13**, and 2.3 Å for **14**. The second method estimates of the gauche migration barriers were much higher. For RHF, they were 60.8 (**12**) to 75.0 kcal/mol (**13**) and for DFT, they were 16.6 (**12**) to 42.1 kcal/mol (**13**).

The large energy differences between the TSG1 estimates and the TSG2 estimates are another indication of the unfavorability of gauche migration. The main difference between TSG1 and TSG2 is the position of the gauche hydrogen or methyl group, since both models include at least partially broken O−O bonds. Thus, the increase in the TSG2 numbers likely results from forcing the gauche group into an approximate transition structure geometry. Both TSG1 and TSG2 lack the stabilizing molecular orbital overlap of the *app* transition structure. Therefore, another factor must also contribute to the destabilization of gauche migration, possibly destabilizing molecular orbital overlaps.

The TSG1 estimates are 11.9 (**11**) to 14.7 kcal/mol (**13**) higher in energy than the *app* transition structures at the RHF level of theory. According to the TSG2 estimates, *app*-migration is favored by 41.4 (**11**) to 44.8 kcal/mol (**13**). Thus, the gauche migration barrier is at least 11.9 kcal/mol higher than the *app*-barrier and could be as much as 44.8 kcal/mol higher. This difference is large enough to guarantee that only *antiperiplanar* migration will be observed.

However, the B3LYP results do not necessarily support the above conclusion and the results are quite different. For one thing, the energy differences between gauche and anti migration are much more system dependent than the RHF values, which were similar for the four model systems. In addition, the calculated energy differences are much smaller. The TSG1 method estimates that the gauche barrier is 1.6 (**12**) to 14.3 kcal/mol (**13**) higher in energy than the *app*-barrier and the TSG2 method estimates differences of 14.0 (**12**) to 33.8 kcal/mol (**13**).

At first glance, these numbers do not necessarily correspond to only *app*-migration. The model system **12** calculations of the gauche barrier give a lower limit of only 1.6 kcal/mol. Thus, some gauche migration may be possible. However, it turns out that the TSG1 method is not a good model of gauche migration for system **12** at the B3LYP level of theory. The *app* transition structure for this model is extremely early with almost no migration occurring and only modest amounts of O−O bond breaking. The C−C−O bond angle in the *app* TS is 97.2°, while the frozen H−C−O angle used for the TSG1 calculation is 98.8°. In this case, the TSG1 structure is actually a good estimate of anti migration rather than gauche migration and has similar energies to the anti

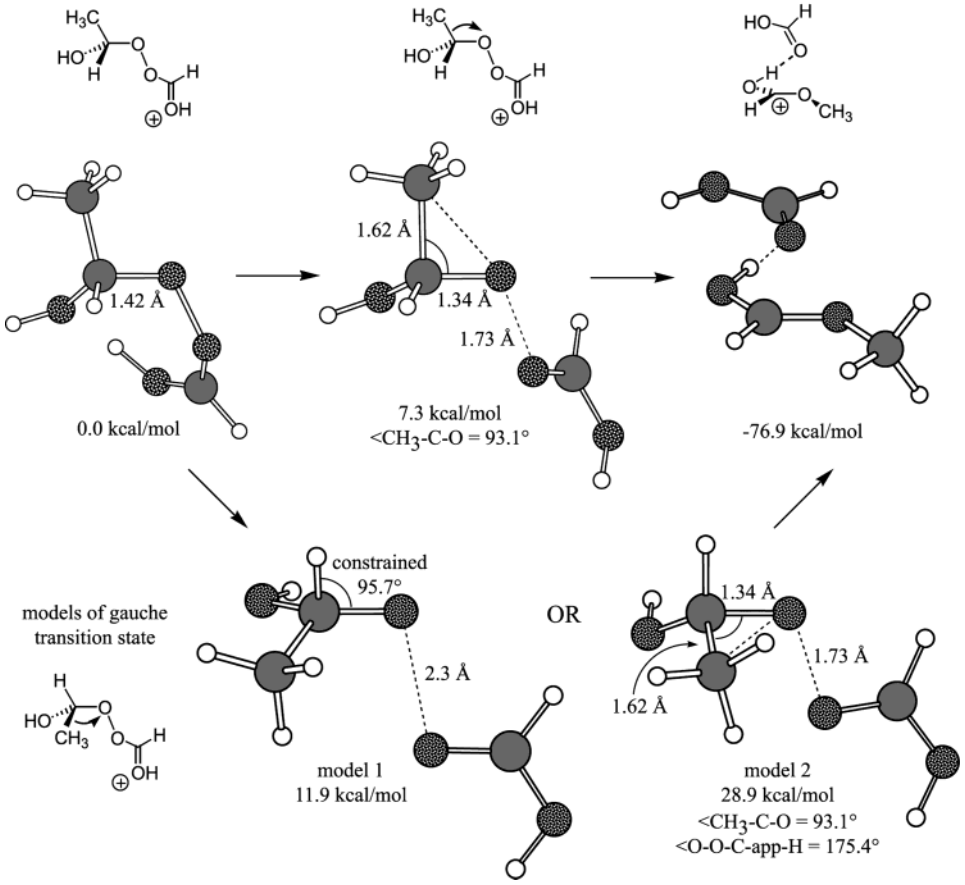

FIGURE 3. B3LYP/6-311G* optimized geometries of acetaldehyde plus peroxyformic acid (**13**) cationic reactant, the antiperiplanar transition state, and the products ($HC(OH)OCH_3^+$ and formic acid). The gauche transition state is approximated by two different model systems.

barriers. The H−C−O angle can be frozen at 105° to lessen the similarity between the TSG1 structure and the *app* transition structure. This gives an estimate of 6.4 kcal/mol for gauche migration, which is 3.8 kcal/mol higher in energy than *app*-migration. This difference is large enough that almost all of the product will result from *app*-migration. The rest of the estimated barriers indicate that gauche migration is highly improbable.

Of interest in the above discussions is that the lowest value of all the ranges mentioned above is almost always from model **12** and the highest from model **13**. This is not unexpected since **12** contains a methyl group, which **11** lacks and which is stabilizing to a cationic system. The formate group in **13**, which is missing from **11**, is an inductive electron-withdrawing group, which is destabilizing to cationic systems. The relative energies for model **14**, which has both the methyl and formyl groups, lie between those of **12** and **13**. A more quantitative study of the effects of the methyl and formate substitutions can be gained by comparing systems **11** to **12** and **13** to **14**, or **11** to **13** and **12** to **14**, respectively. Overall, the methyl group has only a slight effect, while the formate substitution has a much larger effect.

Substitution of hydrogen with methyl causes a reduction in the energy differences between the reactants and products. In the reactant, the cation is not resonance stabilized and the methyl substitution will be more stabilizing than in the products where resonance is possible. At the RHF level of theory, the methyl substitution causes a small decrease in the *app*-barrier as expected. However, this substitution has essentially no effect on the *app*-barrier at the B3LYP level. Using the X−C−O bond angle as an indication of the position of the transition state, substitution with methyl causes an earlier TS at both levels of theory. In most cases, the methyl substitution has a significant effect on the estimation of the gauche barriers, leading to a decrease in the difference between gauche and *app energies*.

Upon formyl substitution, a reduction in the energy differences between the reactants and product complexes is also observed. In this case, the substitution is stabilizing for the reactant due to the possibility of resonance. The formyl group is not part of the cation product and thus probably has little effect on the product relative energy. At both levels of theory, the formyl substitution causes significant increases in the *app*-barrier height and the gauche barrier estimations, as expected. The effect of this on the *app* and gauche barrier differences is random at the RHF level, but causes only increases in this difference at the B3LYP level of theory. The position of the *app* TS is unchanged by formyl substitution at the RHF level of theory, while the formyl TS is much later at the B3LYP level of theory.

Anionic Baeyer−Villiger Rearrangement. The results from the RHF/6-31G* and B3LYP/6-311G* calculations for the anionic model systems are given in Tables

TABLE 3. RHF/6-31G* Relative Energies (kcal/mol) for the Baeyer−Villiger Anionic Reaction for Various Model Systems

	15		16		17		18	
compd	rel *E*	TS Δ*E*	rel *E*	TS Δ*E*	rel *E*	TS Δ*E*	rel *E*	TS Δ*E*
reactant	0.0		0.0		0.0[b]		0.0[b]	
antiperiplanar TS	59.0	0.0	66.4	0.0	32.8	0.0	41.4	0.0
product complex	−69.6[a]		−41.7		−113.9		−79.9	
gauche TS model 1	108.1	49.1	93.9	27.5	N/A		N/A	
gauche TS model 2	135.1	76.1	105.8	39.4	88.3	55.5	94.8	53.4

[a] O−H bond is frozen. [b] No covalent bond between O and C.

TABLE 4. B3LYP/6-311G* Relative Energies (kcal/mol) for the Baeyer−Villiger Anionic Reaction for Various Model Systems

	15		16		17		18	
compd	rel *E*	TS Δ*E*	rel *E*	TS Δ*E*	rel *E*	TS Δ*E*	rel *E*	TS Δ*E*
reactant	0.0		0.0		0.0[b]		0.0[b]	
antiperiplanar TS	27.8	0.0	33.1	0.0	7.2	0.0	14.4	0.0
product complex	−62.9[a]		−38.0		−103.9		−75.3	
gauche TS model 1	45.8	18.0	43.5	10.4	16.7	9.5	16.4	2.0
gauche TS model 2	85.8	58.0	54.9	21.8	36.6	29.4	47.2	32.8

[a] O−H bond is frozen. [b] No covalent bond between O and C.

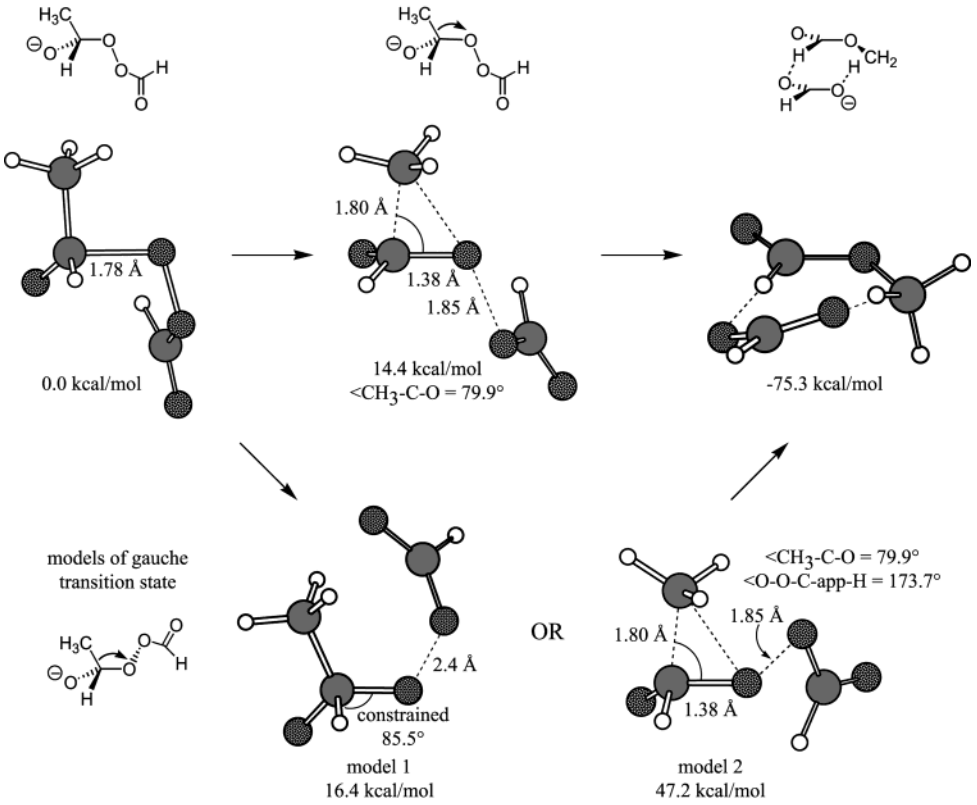

FIGURE 4. B3LYP/6-311G* optimized geometries of acetaldehyde plus peroxyformic acid (**17**) anionic reactant, the antiperiplanar transition state, and the products (methylformate and formate). The gauche transition state is approximated by two different model systems.

3 and 4, respectively. Figure 4 contains the B3LYP/6-311G* anionic geometries of the reactant, the antiperiplanar transition structure, the product complex, the gauche TS1 model, and the gauche TS2 model for acetaldehyde plus peroxyformic acid, **18**. For model system **15**, the initial products, formic acid and hydroxide, undergo a proton transfer to give the more stable complex of formate and water. An estimate of the formic acid−hydroxide complex was achieved by constraining the formic acid O−H bond. For systems **17** and **18**, the O−C bond was broken in the reactants, which were complexes between the peroxyformate and the aldehyde rather than a single molecule. We were unable to locate a single molecule intermediate. The O−C bond is present in the *app* transition structures and all estimates of the gauche transition structures reported in this paper.

A much larger range of values is observed across the four model systems than was observed for the cationic systems. For instance, the anionic products are lower in energy than the reactants by −41.7 (**16**) to −113.9 kcal/mol (**17**) at the RHF/6-31G* level of theory, a difference of 72.2 kcal/mol. The corresponding energies for the cationic systems were only spread over a 20.5 kcal/mol range.

The RHF *app* transition structure barriers range from 32.8 kcal/mol for **17** to 66.4 kcal/mol for **16**. As was the case for the cationic models, the barriers are significantly lower at the B3LYP level of theory, 7.2 (**17**) to 33.1 kcal/mol (**16**). Despite these changes, no effects on the position of the TS were observed. The stretching of the O−O bond to estimate the gauche barrier was unsuccessful for systems **17** and **18** at the RHF/6-31G* level of theory. The bond lengths obtained for **15** and **16** were 2.6 and 2.4 Å, respectively. The resulting barriers were 93.9 kcal/mol for **16** and 108.1 kcal/mol for **15**. The gauche TS1 estimates worked for all four model systems at the B3LYP/6-311G* level of theory. This led to barriers of 16.4 (**18**) to 45.8 kcal/mol (**15**) and O−O bond lengths of 2.7 Å for **15**, 2.5 Å for **16**, 2.25 Å for **17**, and 2.4 Å for **18**. Employing transition structures from the *app*-migration and constraining the O−O−C−*app*-H dihedral angle gave energy barriers from 88.3 (**17**) to 135.1 kcal/mol (**15**). This range drops to 36.6 (**17**) to 85.8 kcal/mol (**15**) at the DFT level of theory. The large differences between the TSG1 estimates and TSG2 estimates observed for the cationic systems are also present for the anionic systems.

The differences in energy between antiperiplanar migration and gauche migration, as estimated by the TSG1 method, were 27.5 kcal/mol for **16** and 49.1 kcal/mol for **15** at the RHF level of theory. The TSG2 estimates predict the *app* transition structure to be lower in energy by 39.4 (**16**) to 76.1 kcal/mol (**15**). These numbers are even larger than those observed for the cationic systems and indicate that only *app*-migration will occur.

Equivalent measurements at the B3LYP level of theory show the *app*-barrier to be favored by 2.0 (**18**) to 18.0 kcal/mol (**15**) with the TSG1 method and by 21.8 (**16**) to 58.0 kcal/mol (**15**) with the TSG2 method. Again, a very low difference between gauche and *app*-migration was observed for the TSG1 method, this time for system **18**. However, in this case, the problem is not caused by the *app* transition structure being very early, as was the case for the cationic system **12**. Here, the problem is that the *anti*-hydrogen is frozen in the reactant position to prevent migration, but because the O−C bond is broken in **17** and **18**, this angle ends up being similar to the *anti*-TS angle of ∼77°. If the H−C−O bond angle is constrained to 105°, a more appropriate sp^3 bond angle, the TSG1 barriers for **17** and **18** are now estimated to be 20.8 and 20.1 kcal/mol. These barriers are 13.6 and 5.7 kcal/mol higher in energy than the corresponding *app*-barriers. Thus, for these anionic systems, the difference between gauche and antiperiplanar migrations is large, ranging from 5.7 to 58.0 kcal/mol at the DFT level of theory.

Unlike the cationic systems, the highest values in the ranges do not come from one particular system, although most of the lowest values come from system **17**. The formate group, missing from system **15**, will be stabilizing under basic conditions. The methyl substitution should also be stabilizing since these systems are in the gas phase. Both methyl and formyl substitutions have large effects on the relative energies. Comparisons between the systems can further establish the effect of these substitutions on the anionic systems.

Methyl substitution causes a decrease in the relative energies between the reactants and products. The substitution is more stabilizing to the reactant than the product because the methyl group is not part of the anionic product molecule. The methyl substitution also causes large increases in the *app*-migration barriers. In the transition state, the migrating methyl group is no longer able to stabilize the anion, increasing the barrier height. Correspondingly, slightly later transition structures are observed for the methyl-substituted systems, based on the X−C−O bond angles. The effect on the gauche migration barriers is mixed from increases, to decreases, to no change. This is not surprising since these structures are not stationary points and the effect of substitutions can thus be unpredictable. For the most part, decreases in the energy differences between the *app* and gauche barriers are observed.

Substitution of formyl causes very large increases in the relative energies between the reactants and products. The formyl group is able to provide resonance stabilization of the anion in the product, but not in the reactant. As a result of the increase in exothermicity, large decreases in the *app*-migration barriers and earlier transition structures are observed. This is in accordance with the Hammond postulate. The gauche barriers are also decreased by formyl substitution; however, in some cases the decrease is larger than for *app* and sometimes it is smaller. This results in random changes in the differences between the *app* and gauche barriers upon formyl substitution.

Comparison of the Cationic and Anionic Systems. For formaldehyde plus peroxide, the reaction of the anionic system is less exothermic by 36 (RHF) or 38 kcal/mol (DFT) compared to the cationic system. This leads to higher energy barriers and a later transition state for the anionic system. It has been demonstrated previously that a poor leaving group causes an increase in the energy barrier of the Baeyer−Villiger reaction.[51,58,59] The cationic system has a good leaving group in water, while the anionic system has a poor one in hydroxide. A similar pattern in the exothermicities and barriers is observed for the cationic and anionic acetaldehyde plus peroxide systems, since they have the same leaving groups, water and hydroxide, respectively.

For formaldehyde plus peroxyformic acid, both the cationic and anionic systems have acceptable leaving groups in formic acid and formate. In this case, the anionic system is more exothermic than the cationic by 20 (RHF) and 15 kcal/mol (DFT). Presumably, the anion product, formate, is better stabilized by resonance than the cation product, $HC(OH)OH^+$. Despite this, little change is observed in the *app*-barriers. As expected, the DFT positive and negative transition structures are at approximately the same stage, though the anionic RHF transition structure is earlier than the cationic.

(58) Winnik, M. A.; Stoute, V. *Can. J. Chem.* **1973**, *51*, 2788.
(59) White, R. W.; Emmons, W. *Tetrahedron* **1962**, *17*, 31.

The addition of a methyl group to the above system should help stabilize the cation product, $HC(OH)OCH_3^+$, but have no effect on the anion product, which is still formate. This should reduce the difference in the exothermicity between the anionic reaction and the cationic one. This hypothesis is supported by the calculations that show little difference in the exothermicity of the two systems (5 kcal/mol RHF, −2 kcal/mol DFT). In contrast, the *app*-barriers are significantly higher for the anionic systems, and correspondingly the transition states are later.

Summary

In both the cationic and anionic systems, antiperiplanar alignment was the only arrangement that led to viable transition states. The unfavorability of gauche migration was emphasized by the nonexistence of transition states for this pathway. Constrained models of gauche migration were used to estimate an energy difference between gauche and anti migration. The latter was found to be lower in energy by at least 3.8 kcal/mol for the cationic system and by at least 5.7 kcal/mol for the anionic system. The B3LYP results indicate that according to the possibly more accurate TSG2 estimates, gauche migration is disfavored by as much as 33.8 kcal/mol for the cationic system and 58.0 kcal/mol for the anionic system. The acetaldehyde plus peroxyformic acid system provides the best model of actual experimental systems. The cationic range for gauche migration was 4.6 to 21.6 kcal/mol and the anionic was 5.7 to 32.8 kcal/mol. Thus, the antiperiplanar migration is also strongly favored energetically and contributes to the observed enantioselectivity of the Baeyer−Villiger reaction. In the antiperiplanar transition structure, there is good orbital overlap between the migrating group and the breaking peroxide bond. As expected, bond breaking cannot be stabilized by orbital overlap in the gauche transition structure and some destabilizing interactions may even be present. This study unambiguously defines the preferred geometry of the Criegee intermediate and provides greater understanding of how stereoselective catalysts for the Baeyer−Villiger reaction work.

Acknowledgment. We thank Dr. Ken Houk for many useful suggestions and discussions. We are grateful to the National Institute of General Medical Sciences, National Institutes of Health, for financial support of this research and the NPACI and San Diego Supercomputer Center for computer time used for this work.

Supporting Information Available: Relative energies and relevant geometrical parameters for reaction and transition state conformers of **11**, **12**, **13**, **14**, **15**, **16**, **17**, and **18** at the RHF and B3LYP levels of theory and B3LYP Cartesian coordinates for the lowest energy conformers. This material is available free of charge via the Internet at http://pubs.acs.org.

JO0491307